Poultry Science®

Changes of bone and articular cartilage in broilers with femoral head necrosis

Hongfan Ge, Yaling Yu, Yanyan Zhang, and Zhenlei Zhou *

Department of Clinical Sciences, College of Veterinary Medicine, Nanjing Agricultural University, Nanjing, Jiangsu, 210095, China

ABSTRACT Femoral head necrosis (**FHN**) in broilers is a common leg disorder in intensive poultry farming, giving rise to poor animal health and welfare. Abnormal mechanical stress in the hip joint is a risk factor for FHN, and articular cartilage is attracting increasing attention as a cushion and lubrication structure for the joint. In the present study, broilers aged 3 to 4 wk with FHN were divided into femoral head separation (**FHS**) and femoral head separation with growth plate lacerations (**FHSL**) groups, with normal broilers as control. The features of the hip joint, bone, and cartilage were assessed in FHN progression using devices including computed tomography (**CT**), atomic force microscope (**AFM**), and transmission electron microscopy (**TEM**). Broilers with FHN demonstrated decreased bone mechanical properties, narrow joint space, and thickened femoral head stellate structures. Notably, abnormal cartilage morphology was observed in FHN-affected broilers, characterized by increased cartilage thickness and rough cartilage surfaces. In addition, as FHN developed, cartilage surface friction and friction coefficient dramatically increased, while cartilage modulus and stiffness decreased. The ultramicro-damage occurred in chondrocytes and the extracellular matrix (**ECM**) of cartilage. Cell disintegration, abnormal mitochondrial accumulation, and oxidative stress damage were observed in chondrocytes. A notable decline in cartilage collagen content was observed in ECM during the initial stages of FHN, accompanied by a pronounced reduction in collagen fiber diameter and proteoglycan content as FHN progressed. Furthermore, the noticeable loosening of the collagen fiber structure and the appearance of type I collagen were noted in cartilage. In conclusion, there was a progressive decrease in bone quality and multifaceted damage of cartilage in the femoral head, which was closely linked to the severity of FHN in broilers.

Key words: femoral head necrosis, extracellular matrix, cartilage, broiler

2024 Poultry Science 103:104127
https://doi.org/10.1016/j.psj.2024.104127

INTRODUCTION

Since 2016, poultry meat production has comprised approximately 40% of the global meat output (Dong et al., 2024), which is attributed to the application of intensive systems in broiler farming (Castro et al., 2023). Nowadays, fast-growing broilers exhibit a 400% growth rate increase compared with the data from 1957 (Zuidhof et al., 2014; Dinev et al., 2019). However, high growth increases the incidence of metabolic diseases including leg disease in broilers (Packialakshmi et al., 2015; Liu et al., 2023). Femoral head necrosis (**FHN**) is a significant leg disease challenge in the poultry farming industry (McNamee et al., 2000; Dinev, 2009), resulting in substantial economic losses (Xu et al., 2022). Femoral head necrosis is a progressive hip disease (Chen et al., 2020) primarily affecting the femoral head (Singh et al., 2023). It is characterized by its collapse of femoral head and damage to the overlying articular cartilage (Guerado et al., 2016). The pathogenesis of FHN is complex. Numerous studies indicated that opportunistic pathogens with hematogenous distribution induce the necrotic degeneration of the femur in broilers (Wideman, 2016; Weimer et al., 2021). Additionally, abnormal lipid metabolism (Quan et al., 2023), impaired osteogenic differentiation (Petek et al., 2019), microcirculatory disorders (Kang et al., 2010), and genetic predisposition (Hines et al., 2021) are also potential pathogenic factors. Recent reports suggest that abnormal mechanical stress in the hip joint is also one of the main causes of femoral head lesions (Elgaz et al., 2020; Tan et al., 2021; Li et al., 2023), and articular cartilage plays a vital role in the hip joint, acting as the specialized structure responsible for load cushioning and lubrication (Alcaide-Ruggiero et al., 2023).

Articular cartilage consists of approximately 3 to 5% chondrocytes and 95% extracellular matrix (**ECM**) (Yu

Received April 23, 2024.
Accepted July 24, 2024.
*Corresponding author: zhouzl@njau.edu.cn

et al., 2024). Chondrocytes secretes ECM, which serves as the material basis for maintaining the structural integrity and biomechanical function of cartilage (Wei et al., 2021; Alcaide-Ruggiero et al., 2023). Articular cartilage damage demonstrates not only ultramicro-damage in chondrocytes and ECM but also alterations in cartilage structure and biomechanics (Kuettner et al., 2005; Li et al., 2022). In FHN-affected broilers, Liu et al. (2021b) indicated that the matrix synthesis capacity of chondrocytes was affected negatively. Zhang et al. (2019) and Yu et al. (2020) demonstrated reduced chondrocyte vitality, enhanced apoptosis, and impaired chondrocyte matrix synthesis capacity in a glucocorticoid-induced FHN model in broilers.

Several studies have been conducted to analyze the characterization of cartilage damage in broilers with FHN. These studies investigated the structure and function of chondrocytes, neglecting the morphological and biomechanical changes in articular cartilage. Therefore, the present study identified the morphology, composition, and mechanical features of the cartilage in the femoral head during the development of FHN in broilers. Furthermore, in this work, we also investigated radiological features of the hip joint and bone phenotype parameters.

MATERIALS AND METHODS

Sample Collection

All animal treatments in the experiment were approved by the Animal Protection and Use Committee of Nanjing Agricultural University (# NJAU-Poult-2023042503, approved on April 25, 2023). The broilers (Arbor Acres broilers) of both sexes were obtained from a farm located in Jiangsu Province. Broilers were provided with ad libitum access to a 2-phase commercial diet: a starter diet (21% CP, 0.6% Ca, 0.5% total P, 0.82% methionine and cystine, 0.3% NaCl) from 0 to 21 d, a grower diet (19% CP, 0.6% Ca, 0.4% total P, 0.71% methionine and cystine, 0.2% NaCl) from 22 d to slaughter. Lame broilers aged 3 to 4 weeks were selected in the present study. After gait scoring (Granquist et al., 2019), body weight (**BW**) was recorded and blood samples were obtained through the wing vein. The serum was isolated and stored at -20°C until analysis. Then, broilers were euthanized by the cervical dislocation method, and computed tomography (**CT**) was used to obtain hip radiological images before pathological dissection. During pathological dissection, the skin covering the hip joint and femur was entirely peeled off, and the exposed muscle tissue was subsequently immersed with 75% ethanol (cat. G73537O, Titan Technology Co., Ltd, Shanghai, China), and the soft tissues around the hip joint were dissected with a sterile scalpel to expose the articular surface of the proximal femur (Al-Rubaye et al., 2015). The proximal femur was assessed based on the FHN score standard (Durairaj, et al., 2009), and then sampled for bacterial cultures at the growth plate of FHN-affected broilers using sterile disposable sampling swabs (cat. SK99-1010-1208, SCHWENK, Ulm, Germany). According to the assessment, the broilers were divided into 2 groups: the femoral head separation (FHS) group and the femoral head separation with growth plate lacerations (**FHSL**) group. Each group had 12 broilers. The cartilage of the femoral head was collected and washed with sterile PBS (**PBS,** cat. G4250-500ML, Servicebio Technology Co., Ltd, Wuhan, China), and the collected cartilage samples were divided into 3 parts, one for histological analysis and reactive oxygen species (**ROS**) measurements, one for TEM and AFM testing, and the other one for macroscopic analysis. In addition, femurs and tibia samples were collected and stored at -20°C after removing all adherent tissues for subsequent analysis. 12 normal broilers were selected as the control group by gait scoring and pathological dissection, with the same sampling method as that of lame broilers.

Computed Tomography Imaging

The broilers were placed in a prone position and a whole-body scan was conducted using the 16 slices computed tomography (**CT**, Hitachi Medical Corporation, Tokyo, Japan). The scanning parameters were 120 kV, 200 mA, 1.25 mm slice thickness, and 1.06 pitch. The bone window (W/L: 1500/300) and tissue window (W/L: 300/40) of the hip joint were reconstructed.

ELISA Analysis

The frozen serum was thawed overnight at 4°C and used for ELISA analysis after all thawing at room temperature. The indicators were quantified according to the instructions of the chicken-specific ELISA kit (Angle Gene Biotechnology Co., Ltd, Nanjing, China). The kits were used to detect bone turnover markers (**BTM**) related to bone metabolism, including bone alkaline phosphatase (**BALP**, cat. ANG-E32226C), tartrate-resistant acid phosphatase 5b (**TRACP-5b**, cat. ANG-E32229C), osteocalcin (**OC**, cat. ANG-E32164C), and C-terminal peptide of type I collagen (**CTX-I**, cat. ANG-E32233C). The kits were also used to detect indicators related to cartilage metabolism factors, including C-telopeptide of type II collagen (**CTX-II**, cat. ANG-E32220C), C-propeptide of type II procollagen (**PIICP**, cat. ANG-E32223C).

Bacterial Isolation

Staphylococcus aureus (***S. aureus***), *Escherichia coli* (***E. coli***), and *Enterococcus* are the main pathogenic microorganisms responsible for FHN in poultry (McNamee et al., 2000; Kense et al., 2011; Szafraniec et al., 2022). Mannitol salt agar (**MSA**, cat. HB4128), MacConkey agar (**MCA**, cat. HB6238), and M-Enterococcus agar (**MEA**, cat. HB8656) purchased from Hopebio Co., Ltd (Qingdao, China) were used to attempt to isolate *S. aureus, E. coli*, and *Enterococcus* respectively,

Table 1. Biochemical identification tests to confirm bacterial species

Bacterial species	Criteria for biochemical identification tests
Staphylococcus aureus	Yellow colony on MSA, Gram staining (Gram+, cocci-shaped), catalase+, coagulase+
Escherichia coli	Pink colony on MCA, Gram staining (Gram-, rod-shaped), IMViC test (indol+, Methyl red+, Voges-Proskauer-, citrate-)
Enterococcus	Red colony on MEA, Gram staining (Gram+), oxidase-, catalase-, KOH-

MSA, Mannitol salt agar; +, positive; MCA, MacConkey agar; −, negative; MEA, M-Enterococcus agar; KOH, potassium hydroxide. IMViC test represents the Indol, Methyl red, Voges-Proskauer, and citrate tests.

and the bacterial species were then identified through further biochemical identification tests (Table 1) (Girijan et al., 2021; Pal et al., 2022; Farizqi et al., 2023).

Bone Morphology and Bone Mineral Density Analysis

Frozen bone samples were thawed overnight at 4°C, and then thawed completely at room temperature. We measured the bone weight, bone length, and the diameter of the midpoint of the bones. Bone index was calculated as bone weight (mg) to body weight (mg) ratio, while the seedor index (Sgavioli et al., 2017) was calculated as bone weight (mg) to bone length (mm) ratio.

Bone mineral density (**BMD**) was measured in well-thawed femurs and tibia by the dual-energy radiograph bone densitometer (MEDIKORS, Gyeonggi, Korea), and the instrument parameter settings and image analysis were consistent with previous studies (Liu et al., 2021c).

Bone Biomechanical Analysis

Fully thawed femurs and tibiae were tested for a three-point bending test using the universal material testing machine (LR10K Plus, Lloyd Instruments Ltd., England, UK). The span of measurement was determined by the bone length and other parameters were set as in previous studies (Liu et al., 2021c).

Macroscopic Analysis of Cartilage

The cartilage of the femoral head can be divided into a high weight-bearing area (**HWA**), and a low weight-bearing area (**LWA**) based on the degree of weight-bearing (Guo et al., 2020). The cartilage samples were cut along the sagittal plane, and sagittal photographs of the cartilage with a scale were taken. The thickness of cartilage HWA and LWA was measured using the Image J software (US National Institutes of Health) (Brown et al., 2019). Subsequently, the BMD of the femoral head cartilage was obtained using the dual-energy radiograph bone densitometer, following the same procedure as the femoral BMD test. Finally, the cartilage sample was weighed to obtain the wet weight and lyophilized by vacuum freeze dryer (LGJ-12D, Sihuan Technology Co., Ltd, Beijing, China) at -80°C to constant weight. The dry weight was obtained by weighing the samples after freeze-drying. The formula for calculating the water content: [(wet weight - dry weight) ÷ wet weight] × 100%.

Histopathological Analysis

Femoral cartilage samples were cut along the sagittal plane, half of them were stored at -80°C for subsequent ROS measurements, and the other half were fixed with 4% paraformaldehyde (**PFA**, cat. G1101-500ML, Servicebio Technology Co., Ltd, Wuhan, China) for histopathological analysis. After fixation, the cartilage samples were decalcified in 10% EDTA (**EDTA**, cat. G1105-500ML, Servicebio Technology Co., Ltd, Wuhan, China) for at least 2 wk. Then the samples were dehydrated and embedded in paraffin, and serially sectioned along the sagittal plane of the cartilage. Four-μm thick sections were cut for Hematoxylin and Eosin (**HE**) staining, Safranin O/fast green staining, Toluidine blue staining, Alcian staining, and Picrosirius red staining.

The average optical density (**AOD**) of Safranin O, Alcian blue, and Toluidine blue was measured to semi-quantify the proteoglycan content in cartilage using Image J software (Saeki Fernandes et al., 2018; Moo et al., 2022). The AOD of Picrosirius red was measured to semi-quantify the collagen content in cartilage using Image J software (Nagai et al., 2015), and collagen fiber typings were observed by a polarized light microscope. For each slice, 3 random areas were selected, and the average values of these images were used for statistical analysis, with slices from 4 animals in each group being analyzed. The same number of sections were evaluated in subsequent immunohistochemistry analysis and ROS measurements.

Immunohistochemical Analysis

Immunohistochemistry was used to detect the ability of chondrocytes to secrete collagen type II (**col2a1**). The 4-μm thick cartilage sections were rehydrated in xylene (cat. C0430530223, Chemical Reagent Co., Ltd, Nanjing, China) and graded concentrations of alcohol, followed by antigen repair in boiling citrate buffer (cat. G1219-1L, Servicebio Technology Co., Ltd, Wuhan, China). Referring to the instructions, the detection was conducted using a horseradish peroxidase/diaminobenzidine immunohistochemistry (**HRP/DAB IHC**) kit (cat. G1215-200T, Servicebio Technology Co., Ltd, Wuhan, China). col2a1 antibody (1:500) (cat. AF6528 Beyotime Biotechnology Co., Ltd, Shanghai, China)

was used. The percentage of col2a1-positive cells was calculated by a double-blind procedure and the criteria for determining positive cells as in a previous study (Yu et al., 2024).

Measurement of Reactive Oxygen Species

The frozen cartilage samples were embedded in optimal cutting temperature compound (**OCT**, cat. G6059-110ML, Servicebio Technology Co., Ltd, Wuhan, China) and serially sectioned to obtain 6-μm thick frozen sections. Dihydroethidium (**DHE**, cat. G6059-110ML, Powerful Biology Technology Co., Ltd, Wuhan, China) is a common fluorescent probe used to detect intracellular ROS levels. The samples were then incubated with DHE at 37°C for 30 min. Following washing with PBS, imaging was performed by confocal microscopy (NikonA1 HD25, Tokyo, Japan). The fluorescence intensity of DHE in the cartilage sections was quantified using Image J software.

Transmission Electron Microscopy Analysis

The Cartilage samples were fixed in 2.5% glutaraldehyde (cat. G1102-100ML, Servicebio Technology Co., Ltd, Wuhan, China) and sections were made using an ultrathin slicer (Leica EM UC7, Wetzlar, Germany). The morphology and structure of chondrocytes and collagen fibers were observed by transmission electron microscopy (**TEM**, HT7700, HITACHI, Tokyo, Japan). The diameter of cartilage collagen fibers was measured using Image J software. 3 areas were randomly for each slice, and the average of the diameters of 50 collagen fibers from each area was calculated for statistical analysis. Slices from 3 animals per group were evaluated.

Atomic Force Microscope Analysis

The surface morphology and biomechanical parameters of the femoral head cartilage were explored by the PF-QNM mode of atomic force microscope (**AFM**, Dimension Icon, Bruker, Massachusetts, USA). A silicon nitride cantilever with a silicon tip (SNL-10, Bruker, Massachusetts, USA) was applied. The frequency of the cantilever ranged from 50 to 80 kHz, with the spring constant ranging from 0.175 to 0.7 N/m, and the deflection sensitivity of 73.30 nm/V. 3 random locations on the cartilage surface were scanned, each with an area of 3×3 μm^2, and 4 samples were selected from each group to be tested. Analysis of roughness, modulus, stiffness, and friction in cartilage was performed by Nanoscope Analysis v.1.70 software. The friction coefficient was calculated as the friction divided by the normal force, and the normal force was calculated in the same manner as in the previous study (Lawrence et al., 2015).

Statistical Analysis

All data were presented as mean ± SEM. Normality tests were conducted on the multiple group data using SPSS software (IBM version 23, NY). The one-way ANOVA test with Tukey's post hoc test was performed for datasets conforming to a normal distribution, and the Kruskal-Wallis test was used for datasets that did not conform to a normal distribution. $P < 0.05$ represents a significant difference, and $P < 0.01$ represents an extremely significant difference. The correlation between FHN scores and the mechanical parameters of cartilage, as well as the correlation between FHN scores and gait scores, was determined by Spearman correlation analysis.

RESULTS

Clinical Investigation

Lameness is one of the most typical clinical manifestations in broilers with FHN. Normal broilers had healthy and flexible limbs (Figure 1A). As the development of the disease, broilers adopted a crouching posture (Figure 1B), which gradually progressed to paralysis (Figures 1C−1D), and ultimately led to difficulty in walking (Figure 1E). In this study, 100 lame broilers were collected, and gait scoring revealed that over 50% of the culled broilers had gait scores recorded as 4 or 5 (Figure 1F). Subsequently, pathological dissection was performed to macroscopically evaluate the femoral head referring to the FHN scoring criteria. We found that the incidence of FHN in lame broilers was 39.00% (Figure 1G). Among the broilers diagnosed with FHN, 33.33% were categorized as examined as the FHS group, and 66.67% as the FHSL group (Figure 1G). The femoral head lesion in the FHS group was manifested as the separation of the femoral head cartilage from the underlying growth plate, but there was no obvious damage within the growth plate (Figure 1I). Moreover, the femoral head lesion in the FHSL group was more severe, manifested as damage to the growth plate and even femoral head collapse and femoral neck fracture (Figure 1J). Culture of proximal femoral growth plates from the FHN-affected broilers yielded 64 identified bacterial strains in 9 of 13 (69.23%) FHS broilers and 23 of 26 (88.46%) FHSL broilers (Figure 1K), and no bacterial strains were isolated from normal broilers. Specifically, 14 bacterial strains were isolated from FHS broilers, including 7 strains of S. aureus (50.00%), 2 strains of E. coli (14.29%), and 5 strains of Enterococcus (35.71%). 50 bacterial strains were isolated from FHSL broilers, including 19 strains of S. aureus (38.00%), 12 strains of E. coli (24.00%), and 19 strains of Enterococcus (38.00%) (Figure 1L).

In addition, the study showed that the highest incidence of FHSL was found in lame broilers with a gait score of 5. but there is no correlation between the gait score and the severity of FHN ($P > 0.05$) (Figure 1M). In this work, CT scans were conducted in normal and

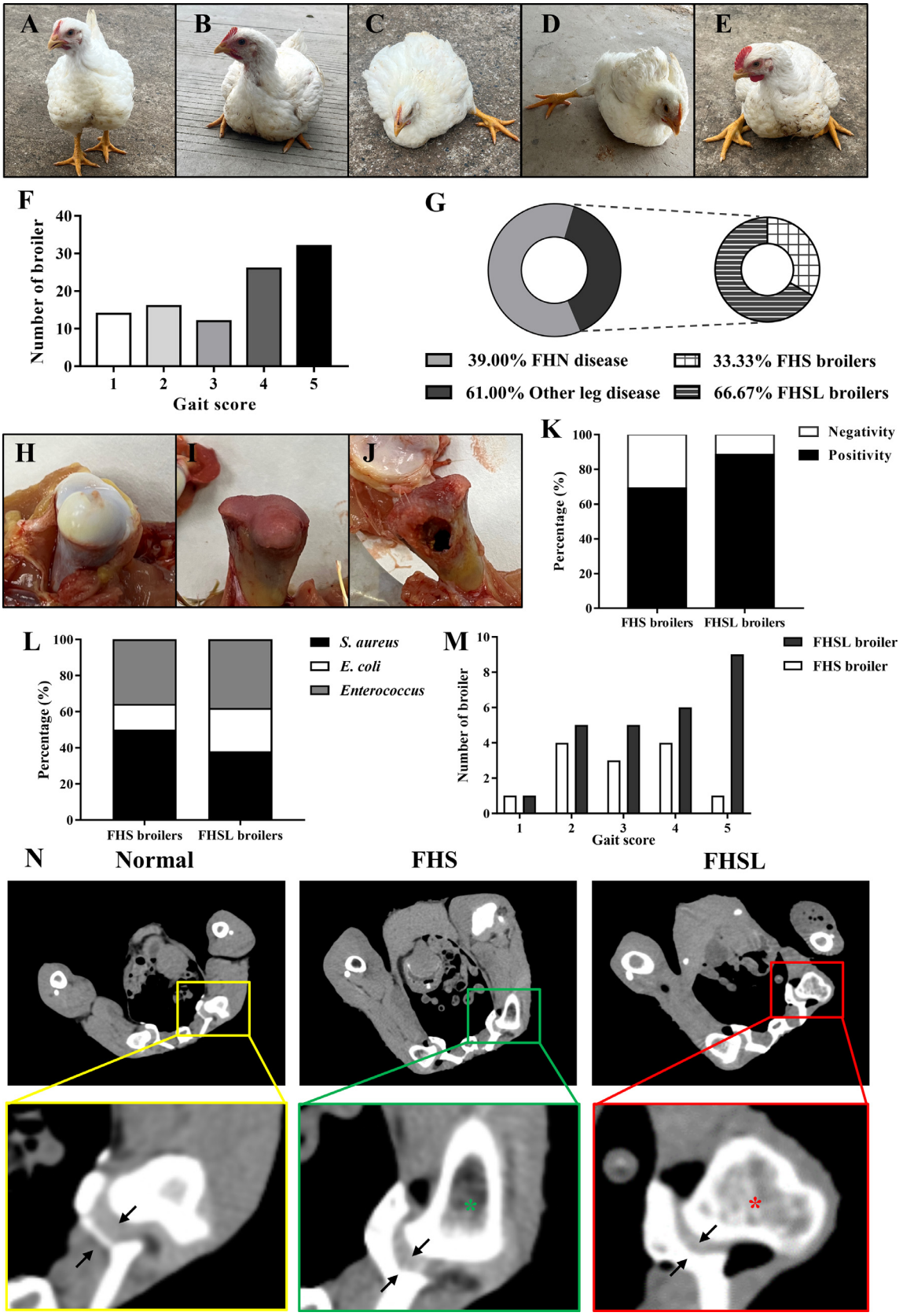

Figure 1. Clinical investigation and radiological features in Broilers with femoral head necrosis. (A) The broiler with normal posture. (B) The broiler with crouching posture. (C) The broiler with a paralyzed left leg. (D) The broiler with a paralyzed right leg. (E) The broiler with paralyzed completely. (F) The number of lame broilers with each gait score. (G) The left circular graph is the percentage of femoral head necrosis (**FHN**) and other leg diseases in lame broilers; The right circular graph is the percentage of femoral head separation (**FHS**) and femoral head separation with growth plate lacerations (**FHSL**) broilers in broilers diagnosed as FHN. (H) Normal femoral head. (I) Femoral head with FHS lesion. (J) Femoral head with FHSL lesion. (K) The positivity and negativity of bacterial cultures from FHS broilers and FHSL broilers. Negativity represents no bacteria isolated from FHS and FHSL broilers; Positivity represents bacteria isolated from FHS and FHSL broilers. (L) The percentage of *Staphylococcus aureus* (***S. aureus***), *Escherichia coli* (***E.coli***), *and Enterococcus* in bacterial isolates from FHS and FHSL broilers. (M) The number of FHS broilers and FHSL broilers with each gait score. (N) Radiographic images of the hip joint (from computer tomography) in FHS, FHSL, and normal broilers. The distance between the 2 black arrows represents the joint space; The green asterisk represents irregular mesh stellate structure in the femoral head, and the red asterisk represents thickened stellate structures in the femoral head.

Table 2. Changes in bone mechanical parameters of the femur and tibia.

Items	Groups			*P* value
	Normal	FHS	FHSL	
Femoral measurements				
Stiffness (N/mm)	113.99 ± 4.44	111.23 ± 6.57	101.12 ±4.17	0.233
Elastic modulus (GPa)	1.82 ± 0.17[a]	1.87 ± 0.21[a]	1.21 ± 0.10[b]	0.052
Yield force (N)	145.97 ± 13.36[a]	103.73 ± 13.22[ab]	97.42 ± 14.63[b]	0.057
Ultimate force (N)	146.36 ± 13.22	110.23 ± 16.38	117.55 ± 10.15	0.177
Yield stress (MPa)	40.43 ± 13.73[a]	51.84 ± 10.09[a]	10.85 ± 1.63[b]	0.013
Ultimate stress (MPa)	40.68 ± 13.89[ab]	55.54 ± 12.36[a]	13.09 ± 1.13[b]	0.017
Tibial measurements				
Stiffness (N/mm)	110.26 ± 4.72	87.50± 4.26	76.40 ± 4.79	0.098
Elastic modulus (GPa)	1.96 ± 0.14	1.70 ± 0.16	1.52 ± 0.19	0.172
Yield force (N)	107.23 ± 4.17[a]	92.56 ± 7.77[ab]	83.44 ± 5.95[b]	0.046
Ultimate force (N)	107.70 ± 4.41[a]	94.24 ± 7.36[ab]	85.62 ± 4.90[b]	0.045
Yield stress (MPa)	52.72 ± 13.64[a]	59.37 ± 10.15[a]	20.87 ± 2.51[b]	0.006
Ultimate stress (MPa)	53.10 ± 13.88[a]	60.74 ± 10.38[a]	21.35 ± 2.29[b]	0.006

n = 8, n indicates the number of biologically independent samples per group. Data are all shown as mean ± SEM.
[a–b]Means with different superscripts within a row differ ($P < 0.05$).

FHN-affected broilers respectively. The results demonstrated that the femoral head of healthy broilers was smooth and rounded; the femoral head of FHS broilers was slightly flattened with irregular mesh stellate structures; while the stellate structures in the femoral head of broilers with FHSL exhibited pathological thickening and distortion (Figure 1N). In addition, FHN-affected broilers all demonstrated varying degrees of joint space narrowing (Figure 1N).

Changes in Bone Parameters of the Femur and Tibia

In the present study, we measured BW and the bone parameters in FHN-affected broilers, including bone morphology, BMD, and bone mechanical parameters. The findings indicated an adverse impact on bone biomechanical functions, especially affecting the parameters related to force (including ultimate load and yield load) and stress (including ultimate stress and yield stress). Notely, the yield load, ultimate stress, and yield stress of the femur of FHSL broilers decreased ($P < 0.05$), while the yield load, ultimate load, ultimate stress, and yield stress of the tibia also decreased ($P < 0.05$). Furthermore, the elastic modulus of the femur in FHSL broilers exhibited the same declining trend ($P < 0.05$) (Table 2).

In this study, the results indicated that the BW of FHSL broilers decreased significantly, compared to FHS and normal broilers. We also investigated the morphological parameters of the femur and tibia. The data demonstrated that no significant changes were observed in bone weight, bone index, bone diameter, bone length, and seeder's index between FHS and FHSL broilers. ($P > 0.05$) (Table 3). Moreover, the BMD of the femur and tibia were negatively affected in FHN. Specifically, the BMD of the femur in FHSL broilers was lower than that of healthy broilers ($P < 0.01$), while the BMD of the tibia in both FHS and FHSL broilers showed a significant decrease ($P < 0.01$) (Table 3).

Table 3. Changes in bone morphology and bone density of the femur and tibia

Items	Groups			*P* value
	Normal	FHS	FHSL	
Body weight (kg)	1.45 ± 0.01[a]	1.43 ± 0.01[a]	1.36 ± 0.02[b]	0.001
Femoral measurements				
Weight (g)	4.13 ± 0.44	3.57 ±0.24	3.21 ± 0.41	0.236
Bone index (%)	0.28 ± 0.03	0.25 ± 0.02	0.23 ± 0.03	0.354
Length (cm)	4.69 ± 1.54	4.72 ± 1.04	4.44 ± 1.86	0.372
Width (mm)	6.03 ± 0.31	5.85 ± 0.15	5.65 ± 0.34	0.581
Seedor's index	88.12 ± 9.53	75.47 ± 4.49	71.08 ± 6.98	0.253
BMD (g/cm^2) [1]	0.15 ± 0.003[a]	0.13 ± 0.007[ab]	0.12 ± 0.005[b]	0.001
Tibial measurements				
Weight (g)	6.10 ± 0.67	5.23 ± 0.33	4.73 ± 0.59	0.224
Bone index (%)	0.42 ± 0.04	0.37 ± 0.02	0.34 ± 0.04	0.336
Length (cm)	7.51 ± 2.10	7.16 ± 1.85	6.75 ± 2.75	0.083
Width (mm)	5.76 ± 0.34	5.19 ± 0.16	5.15 ± 0.34	0.285
Seedor's index	80.16 ± 6.91	72.64 ± 3.52	68.32 ± 6.08	0.349
BMD (g/cm^2) [1]	0.14 ± 0.002[a]	0.12 ± 0.005[b]	0.12 ± 0.005[b]	0.001

n = 8, n indicates the number of biologically independent samples per group. Data are all shown as mean ± SEM.
[1]BMD indicates bone mineral density.
[a–b]Means with different superscripts within the same row differ ($P < 0.05$).

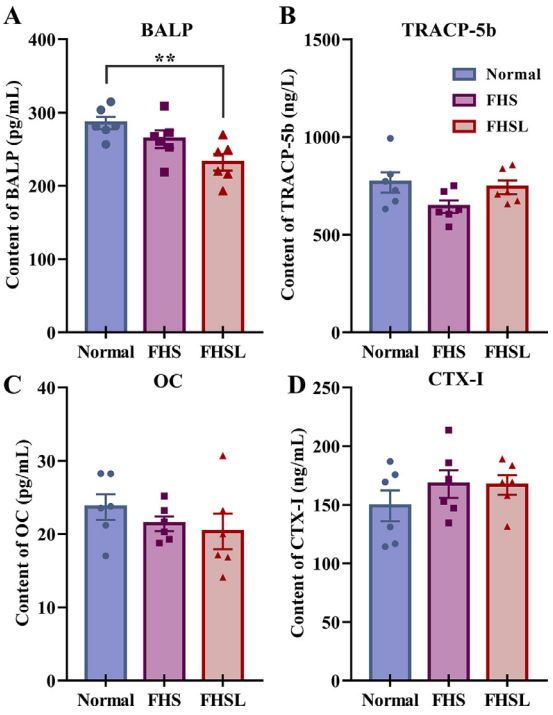

Figure 2. Changes in bone turnover markers in broilers with FHN. (A) The content of bone alkaline phosphatase (**BALP**) in serum, n = 6. (B) The content of tartrate-resistant acid phosphatase 5b (**TRACP-5b**) in serum, n = 6. (C) The content of osteocalcin (**OC**) in serum, n = 6. (D) The content of C-terminal peptide of type I collagen (**CTX-I**) in serum, n = 6. Data are all shown as mean ± SEM. n indicates the number of biologically independent samples per group. $^{*}P < 0.05$, $^{**}P < 0.01$.

Changes in Bone Turnover Markers

Subsequent investigations focused on the alterations in bone turnover markers (**BTM**) between FHN-affected broilers and normal broilers. These results revealed a significant reduction in bone formation-related marker BALP content in FHSL broilers ($P < 0.01$) (Figure 2A), while other BTM did not change significantly($P > 0.05$) (Figure 2B−2D).

Cartilage Macromorphological Observation

The articular cartilage serves as the load-bearing and cushioning barrier of the femur. FHN is closely related to high load, and the changes in femoral cartilage during the development of FHN in broilers are of interest. The schematic diagram of HWA and LWA in the femoral head cartilage is depicted in Figure 3A. Our study revealed a thickening trend in femoral head cartilage during the development of FHN, with the cartilage thickness in both HWA and LWA increasing substantially in FHSL broilers compared to healthy broilers ($P < 0.05$) (Figure 3B−3C). Interestingly, despite this thickening, the BMD of the femoral head cartilage decreased in FHSL broilers ($P < 0.05$) (Figure 3D). The water content of cartilage increased in FHSL broilers, but not significantly compared to that of normal broilers ($P > 0.05$) (Figure 3E). Furthermore, the cartilage metabolism marker PIICP was elevated in FHS broilers ($P < 0.01$). Still, there was no significant difference in PIICP content between FHSL broilers and healthy broilers ($P > 0.05$) (Figure 3F), and no significant difference in CTX-II content between FHN broilers and normal broilers ($P > 0.05$) (Figure 3G).

Cartilage Micromorphological and Biomechanics Observation

To further investigate cartilage characteristics in FHN-affected broilers, cartilage surface morphology and biomechanical function at the nanoscope were studied using ATM. The three-dimensional surface topography of the femoral head cartilage in FHN-affected broilers is depicted in Figure 4A. We found that the micro-surface fluctuations of broiler femoral head cartilage in normal broiler were below 50 nm, while those in FHS and FHSL broilers ranged from 50 to 100 nm (Figure 4A). The color variations indicated that the surface fluctuation interval of femoral head cartilage was small in normal broiler, suggesting a smoother micro-surface. Furthermore, with the progression of FHN, local bulges on the micro-surface of cartilage were gradually higher, and the percentage of bulge area progressively expanded, suggesting that the micro-surface of cartilage becomes roughened (Figure 4A). As illustrated in Figure 4B, the surface roughness of the femoral head cartilage in FHSL broilers was significantly higher than that in FHS broilers and healthy broilers ($P < 0.01$), consistent with the findings of three-dimensional morphology analysis. HE staining results also indicated varying degrees of structural damage at the edge of the femoral head cartilage in FHN-affected broilers (Figure 4C).

The stiffness and modulus of the femoral head cartilage in FHS and FHSL broilers were significantly lower than those of normal broilers ($P < 0.01$) (Figures 4D−4E). The friction coefficients of the cartilage in healthy broilers ranged from 0.003 to 0.006 (Figure 4F−4G), whereas those in FHS and FHSL broilers ranged from 0.006 to 0.010 and 0.015 to 0.073, respectively. Additionally, both the friction and friction coefficient of femoral head cartilage increased with the progression of FHN ($P < 0.01$) (Figures 4F−4G). By correlation analysis, we found a strong positive correlation between the FHN score, representing the severity of FHN, and the cartilage's surface roughness, friction force, and friction coefficient ($0.90 \leq r \leq 0.94$, $P < 0.01$) (Figure 4H). Conversely, there was a strong negative correlation between the FHN score and cartilage stiffness ($r = -0.78$, $P < 0.01$), and a moderate negative correlation with cartilage modulus ($r = -0.70$, $P < 0.01$) (Figure 4H). Furthermore, a moderate positive correlation was found between cartilage stiffness and modulus ($r = 0.62$, $P <$

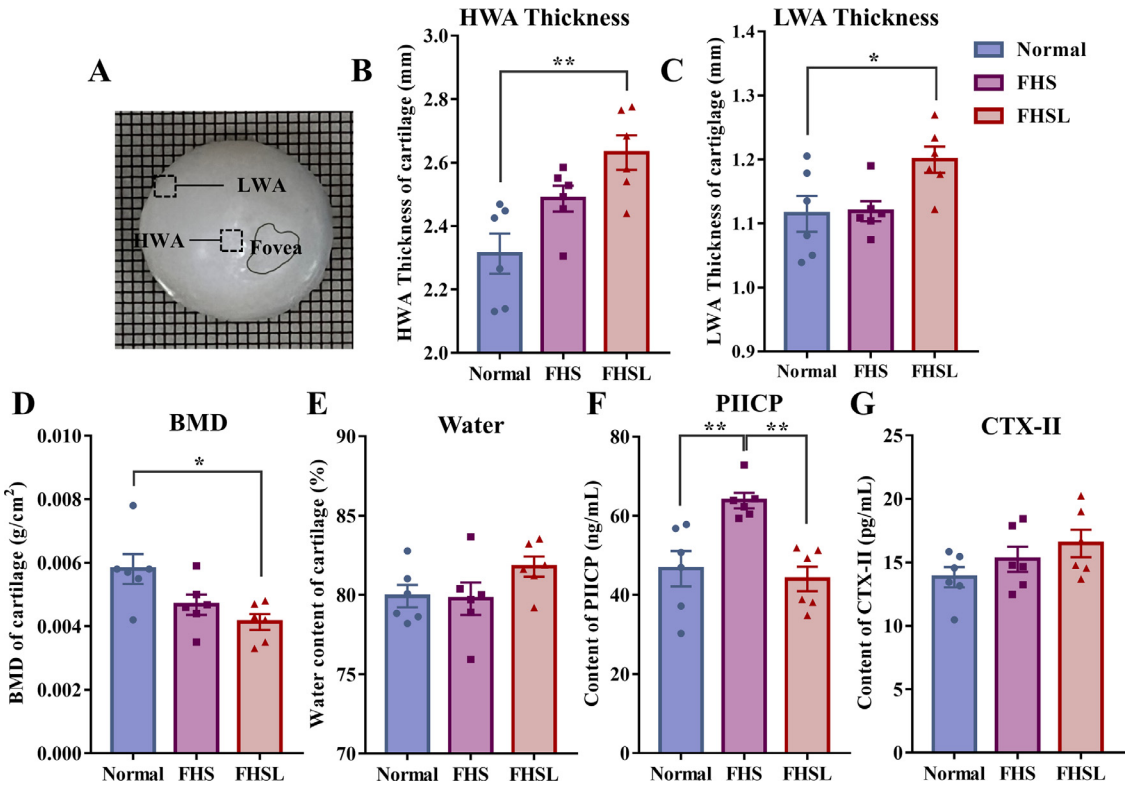

Figure 3. Macroscopic changes in femoral head cartilage in broilers with FHN.(A) Schematic illustration of the high weight-bearing area, (**HWA**) and low weight-bearing area (**LWA**) in femoral head cartilage in broilers. The fovea represents the fovea capitis femoris. (B) HWA thickness of femoral head cartilage, n = 6. (C) LWA thickness of femoral head cartilage, n = 6. (D) Bone mineral density (**BMD**) of femoral head cartilage, n = 6. (E) The water content of femoral head cartilage, n = 6. (F) The content of C-propeptide of type II procollagen (**PIICP**) in serum, n = 6. (G) The content of C-propeptide of C-telopeptide of type II collagen (**CTX-II**) in serum, n = 6. Data are all shown as mean ± SEM. n indicates the number of biologically independent samples per group. $^{*}P < 0.05$, $^{**}P < 0.01$.

0.01), and a strong positive correlation existed among cartilage roughness, friction force, and friction coefficient ($0.88 \leq r \leq 0.99$, $P < 0.01$) (Figure 4H). In addition, there was a negative correlation between stiffness and roughness, friction, and friction coefficient respectively ($-0.79 \leq r \leq -0.71$, $P < 0.01$), and a moderate negative correlation between modulus and roughness, friction, and friction coefficient respectively ($-0.67 \leq r \leq -0.56$, $P < 0.01$) (Figure 4H).

Chondrocytes Ultrastructural Observation and ROS Generation

TEM was used for observing the ultrastructural changes of chondrocytes. The TEM analysis revealed that chondrocytes of normal broilers exhibited an elliptical morphology, with intact cell membranes, protrusions around the membrane, and abundant rough endoplasmic reticulum in the cytoplasm. The morphology of chondrocytes in FHS broilers was generally normal, with appearing organelle cavitation and typical autophagosomes. Additionally, the chondrocytes in FHSL broilers appeared cellular swelling, with membrane disruption, nuclear deformation, and numerous abnormal mitochondria accumulation in the cytoplasm (Figure 5A). HE staining showed a gradual deepening of intracytoplasmic vacuolization in chondrocytes with the development of FHN (Figure 5B). Furthermore, the results indicated that the accumulation of ROS in chondrocytes increased significantly ($P < 0.01$) as the FHN progressed (Figures 5C −5D).

Cartilage ECM Structure and Composition Analysis

The ECM serves as the material basis for the structure and biological functions of cartilage, primarily composed of proteoglycans and collagen fibers. Semi-quantitative analysis of cartilage proteoglycan content was conducted using Safranin O/fast green staining, Toluidine blue staining, and Alcian blue staining (Schmitz et al., 2010; Sun et al., 2012). The results demonstrated that proteoglycans were gradually lost in the ECM as the FHN developed, and the proteoglycan content of the cartilage ECM in FHSL broilers was significantly lower compared to those of normal broilers ($P < 0.01$) (Figures 6A−6F). Additionally, the cartilage proteoglycan content of FHSL broilers was greatly lower than that of FHS broilers ($P < 0.05$) (Figures 6C−6D).

The TEM analysis indicated that collagen fibers were abundant and tightly arranged in the cartilage ECM of normal broilers. The cartilage collagen fibers in FHS

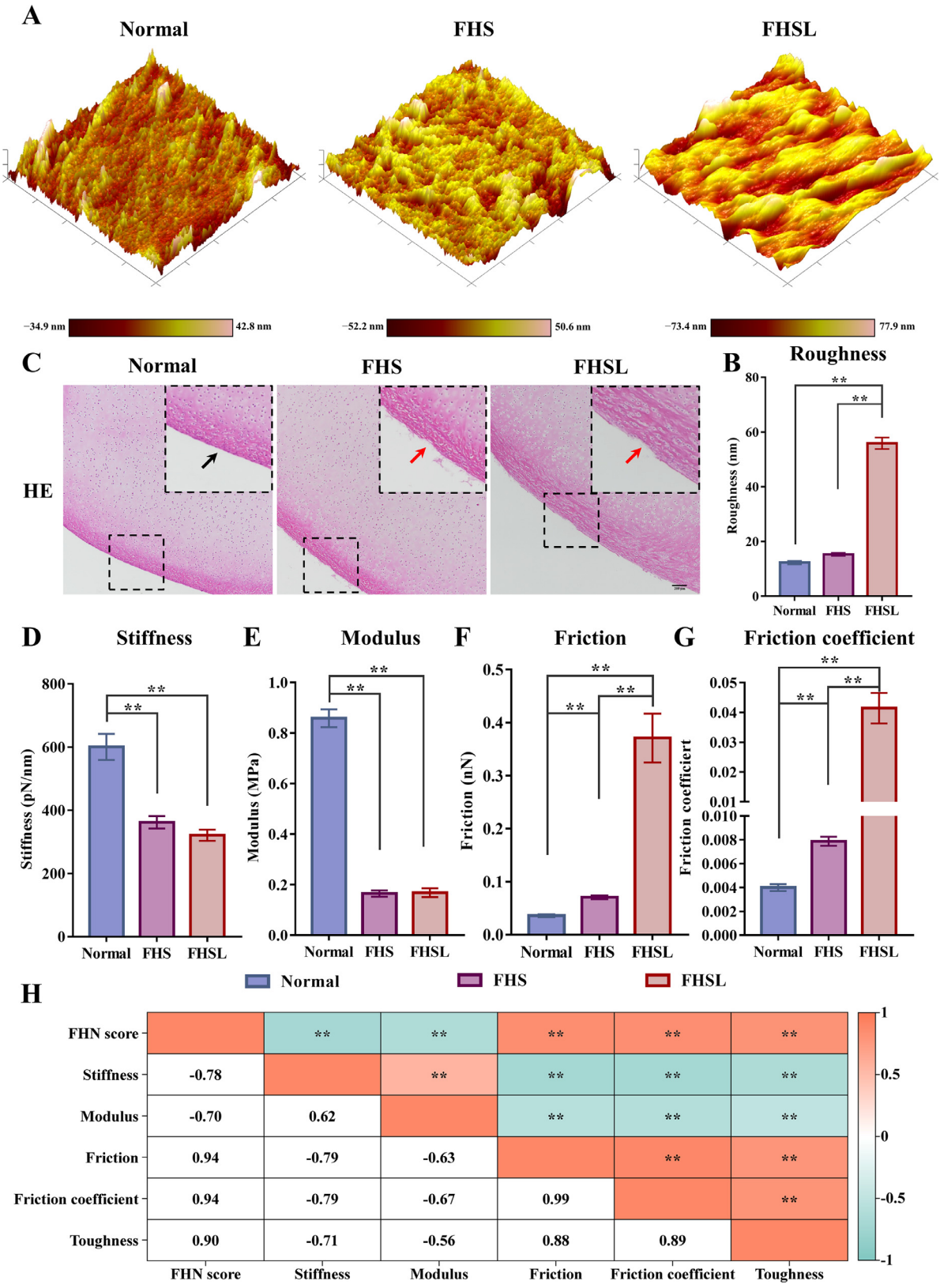

Figure 4. Changes in micromorphological and Biomechanics of cartilage surface in broilers with FHN. (A) The three-dimensional surface topography of femoral head cartilage in normal, FHS, and FHSL broilers, each image from an area of $3 \times 3\ \mu m^2$. (B) The surface roughness of the femoral head cartilage, n = 4. (C) Hematoxylin and Eosin (**HE**) staining of femoral head cartilage in normal, FHS, and FHSL broilers, n = 4, bar = 200 μm. The right top panels are higher-resolution pictures of the cartilage outline in the black dashed boxes. The black arrow represents the intact cartilage surface, red arrows represent damaged cartilage surfaces. (D) The surface stiffness of the femoral head cartilage, n = 4. (E) The surface modulus of the femoral head cartilage, n = 4. (F) The surface friction of the femoral head cartilage, n = 4. (G) The surface friction coefficient of the femoral head cartilage, n = 4. (H) Pearson correlation heat map between FHN score and cartilage mechanical properties and surface roughness. $^{*}P < 0.05$ and $^{**}P < 0.01$ indicate statistically significant correlations between the two variables and the numbers in the heat map are the Pearson correlation coefficients (r) between the two variables. Data are all shown as mean ± SEM. n indicates the number of biologically independent samples per group. $^{*}P < 0.05$, $^{**}P < 0.01$.

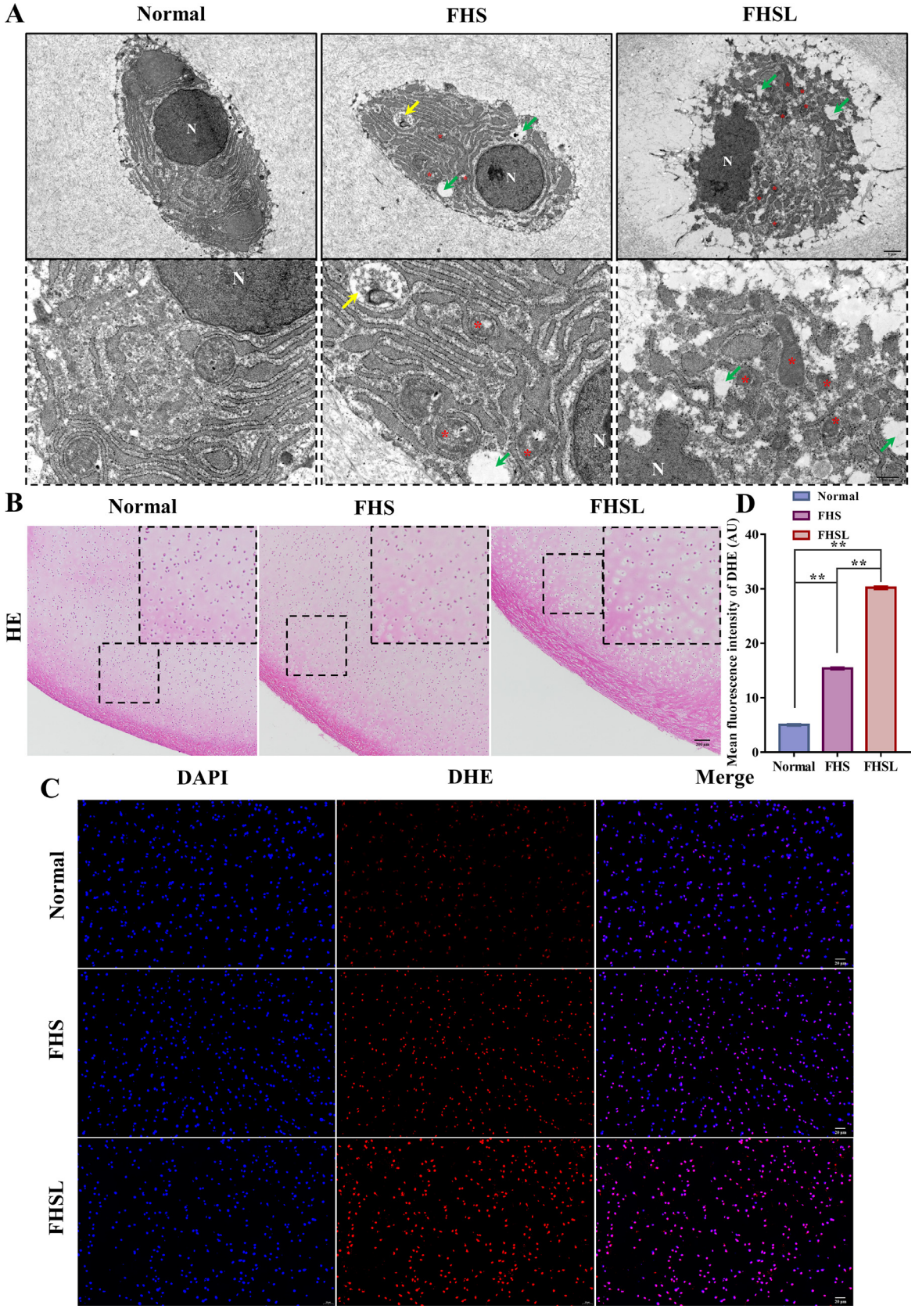

Figure 5. Changes in chondrocytes ultrastructure and reactive oxygen species levels in broilers with FHN. (A) Transmission electron microscope (**TEM**) images of chondrocytes ultrastructure in normal, FHS, and FHSL broilers, n = 3. The first row displays the TEM images of chondrocytes at 3,000 ×, bar = 1 μm, and the second row displays the TEM images at 8,000 × of the same chondrocytes in the image above, bar = 500 nm. N indicates nucleus; yellow arrows represent autophagosome; green arrows represent organelle cavitation; red asterisks represent abnormal mitochondria, characterized by abnormal morphology, vacuoles, and indistinct mitochondria borders. (B) HE staining of femoral head cartilage in normal, FHS, and FHSL broilers, n = 4, bar = 200 μm. The right top panels are higher-resolution pictures in the black dashed boxes. (C) The reactive oxygen species (**ROS**) levels of chondrocytes in normal, FHS, and FHSL broilers, n = 4, bar = 20 μm. DAPI (blue) marks the nucleus; fluorescent probe Dihydroethidium (**DHE**) (red) marks intracellular ROS. (D) The mean fluorescence intensity of DHE in groups. Data are all shown as mean ± SEM. n indicates the number of biologically independent samples per group. $^{*}P < 0.05$, $^{**}P < 0.01$.

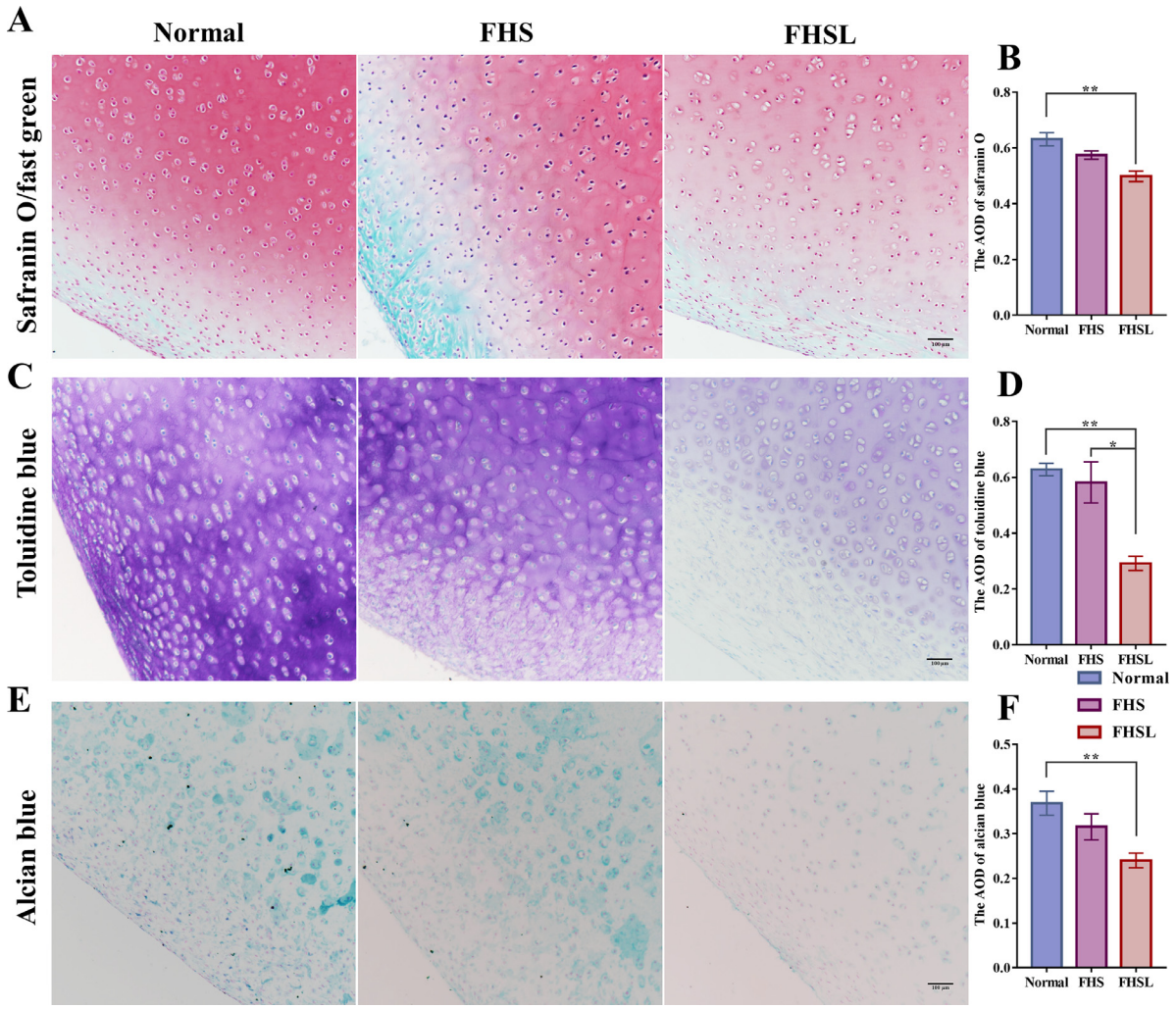

Figure 6. Changes in proteoglycan content of cartilage in broilers with FHN. (A) Safranin O/fast green staining of femoral head cartilage in normal, FHS, and FHSL broilers, n = 4, bar = 100 μm. (B) The average optical density (**AOD**) of Safranin O in groups. (C) Toluidine blue staining of femoral head cartilage in normal, FHS, and FHSL broilers, n = 4, bar = 100 μm. (D) The AOD of Toluidine blue in groups (E) Alcian blue staining of femoral head cartilage in normal, FHS, and FHSL broilers, n = 4, bar = 100 μm. (F) The AOD of Alcian blue in groups. Data are all shown as mean ± SEM. n indicates the number of biologically independent samples per group. $^*P < 0.05$, $^{**}P < 0.01$.

broilers were similar to those observed in healthy broilers, while the density of cartilage collagen fibers in FHSL broilers decreased and loosely arranged (Figure 7A). We found that the diameter of cartilage collagen fibers in normal broilers ranged from 8 to 25 nm, with an average diameter of 15.59 nm. The diameter of collagen fibers in FHS and FHSL broilers ranged from 7 to 38 nm and 8 to 17 nm, respectively, with average diameters of 14.15 nm and 11.84 nm (Figure 7B). These data revealed that the diameter of cartilage collagen fibers gradually decreased during the development of FHN, with those in FHSL broilers notably reducing compared to that in normal broilers (Figures 7A−7B) ($P < 0.01$). Picrosirius Red staining, a widely used method for visualizing collagen fibers, revealed that the content of cartilage collagen fiber in FHS and FHSL broilers significantly reduced compared to that in normal broilers and decreased rapidly as the FHN progressed (Figures 7C−7D) ($P < 0.01$).

ECM contains abundant type II collagen in normal cartilage. Synthesis of type II collagen in FHS broiler cartilage was inhibited ($P < 0.05$), and the degree of inhibition gradually deepened with the development of FHN ($P < 0.01$) (Figures 7E−7F). Furthermore, observing picrosirius red stained cartilage under a polarized light microscope, we found that the area of green birefringence gradually increased with the development of FHN, and obvious yellow birefringence was observed in FHSL broilers, suggesting that the composition of cartilage collagen fibers altered (Figure 7G).

DISCUSSION

FHN is the most common skeletal disease in rapidly growing broilers. Currently, FHN studies are mainly performed in FHN models from glucocorticoid injection (Zhang et al., 2019) and wire floor systems (Alrubaye et al., 2020). However, this study focused on the broilers with spontaneous FHN in a poultry farm and demonstrated the pathological changes in bone and cartilage. The radiographic features of the femoral head in broilers

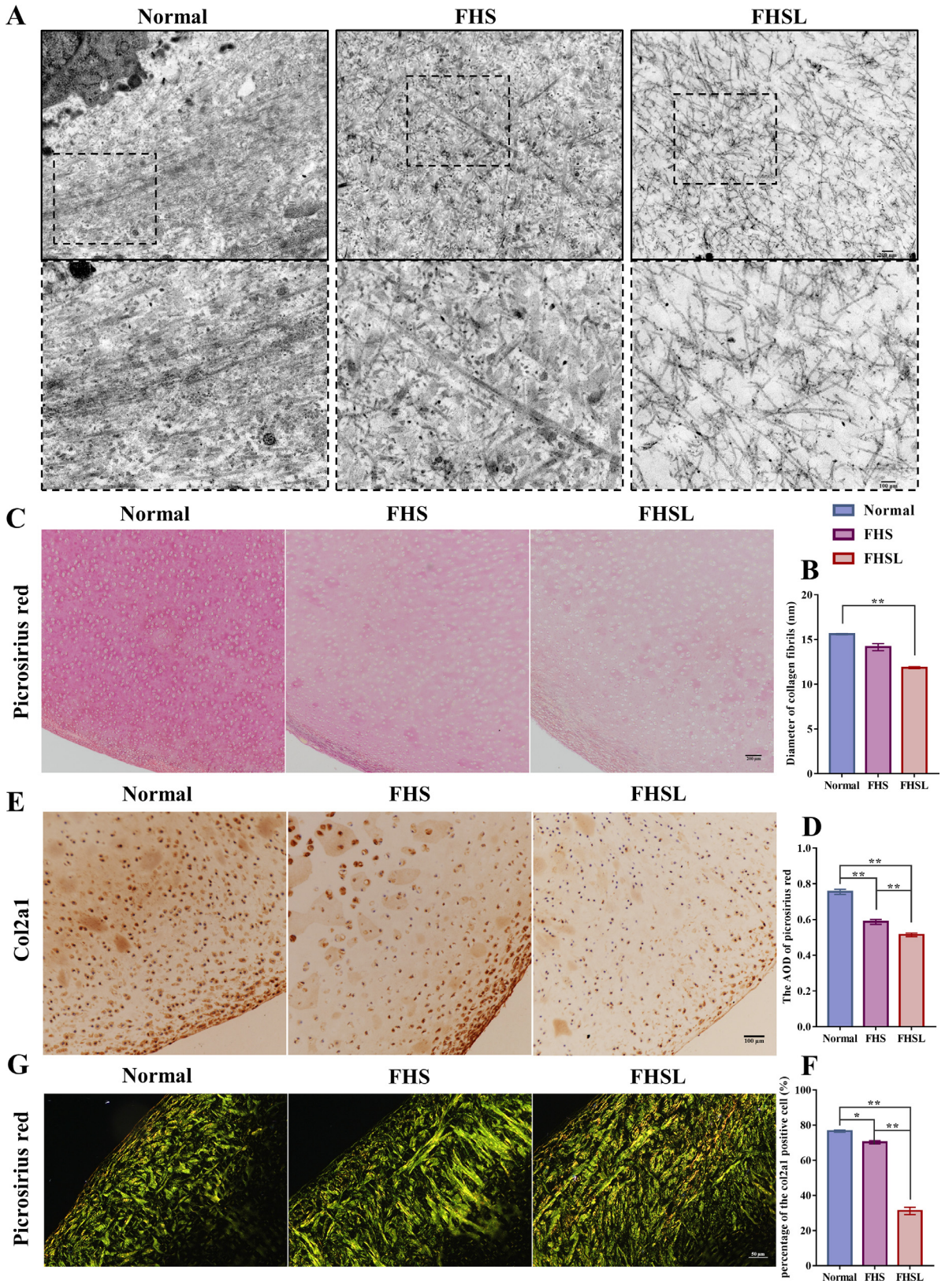

Figure 7. Changes in structure and composition of collagen fibers in cartilage in broilers with FHN. (A) TEM images of collagen fibers in cartilage in normal, FHS, and FHSL broilers, n = 3. The first row displays the TEM images of collagen fibers in cartilage at 8,000 ×, bar = 200 nm, and the second row displays the TEM images at 20000 × of the area in the black dashed box in the above figure, bar = 100 nm. (B) The diameter of collagen fibers in cartilage. (C) Picrosirius red staining of femoral head cartilage in normal, FHS, and FHSL broilers with light microscopy, n = 4, bar = 200 μm. (D) The AOD of Picrosirius red in groups. (E) Immunohistochemical results of col2a1 in cartilage in normal, FHS, and FHSL broilers, n = 4, bar = 100 μm. (F) The percentage of the col2a1 positive cell in groups. (G) Picrosirius red staining of femoral head cartilage in normal, FHS, and FHSL broilers with the polarized light microscope, n = 4, bar = 50 μm. Data are all shown as mean ± SEM. n indicates the number of biologically independent samples per group. $^{*}P < 0.05$, $^{**}P < 0.01$.

with FHN were observed using the CT scanner. At the early stage of FHN in broilers, the morphology of the femoral head showed slight flattening, followed by a gradual narrowing of the joint space, which was similar to the imaging characteristics observed in humans diagnosed with late-stage (stage IV) osteonecrosis of the femoral head (Zhao et al., 2020b). In addition, the trabeculae showed pathological thickening due to excessive compression and stretching, exhibiting uneven stellate structures in the femoral head of FHN broilers. This is consistent with the CT imaging characteristics reported by Murphey et al. (2014) and Chen et al. (2022) in the early stages of FHN in humans. The morphological changes in the femoral head already present in the early stages of FHN may be related to the rapid linear weight gain of broilers (Paz et al., 2009). This also suggested that there may be unique pathological change patterns in the femoral heads during the development of broilers with FHN, which differ from those in humans.

Bone provides crucial mechanical support for the body, and many studies have reported a close association between bone mechanical properties and skeletal diseases (Ma et al., 2022). The present study similarly demonstrated negative changes in the mechanical properties in FHN broilers, with decreased elastic modulus, yield load, yield stress, and ultimate stress in FHSL broilers. Our data indicated that FHN negatively affected the bone strength and resistance to elastic deformation of broiler femurs, potentially contributing to femoral head and femoral neck fractures. Liu et al. (2021c) and Fan et al. (2021) indicated that BMD of the femur and tibia in broilers was adversely influenced by FHN. In the present study, the BMD of the long bones in broilers with FHN was significantly reduced, consistent with previous studies. Nobakhti et al. (2018) demonstrated that approximately 70% of the changes in bone elastic modulus in osteoporosis could be attributed to BMD. Therefore, decreased BMD of the long bones in broilers with FHN may be a reason for the change in bone elastic modulus. In addition, this study found a significant decrease in BW of FHSL broilers, associated with the difficulty faced by lame broilers in obtaining feed and water (Szafraniec et al., 2022). BW is considered a potential factor in bone regulation (Grupioni et al., 2015). Lilburn et al. (1989) reported that bone growth was closely related to BW in broiler feeding. Similarly, Kolakshyapati et al. (2019) demonstrated that heavier hens had greater bone size and ultimate load in the tibia. Therefore, the low BW of FHSL broilers may be relevant to poorer bone mechanical properties and bone size. FHS broilers had lower BMD and bone mechanical properties, despite having similar BW to normal broilers, which might be induced by alterations in osteoblasts and osteoclasts (Wang et al., 2018). BTM, including markers for bone formation and resorption, reflects osteoblast and osteoclast activities.

BTM in serum is commonly used to evaluate bone health (Zhao et al., 2020a). Bone remodeling is in dynamic equilibrium (Bolamperti et al., 2022). BALP in BTM is regarded as one of the most accurate indicators of bone formation (Liu et al., 2021c). In this study, the content of BALP decreased, while the rest of the BTM showed no significant changes compared with healthy broilers, suggesting imbalanced bone remodeling and bone metabolism disorders in broilers with FHN. Bone mechanical properties, BMD, and bone turnover are methods used to assess bone quality (Kuroshima et al., 2017; Wang et al., 2022). In this present study, it was indicated that a progressive decrease in bone quality was observed in broilers with FHN.

The femoral head is the primary site of FHN lesions in broilers, covered by articular cartilage (Yu et al., 2024). Our study revealed that compared to healthy cartilage, both the thickness of HWA and LWA cartilage increased in FHSL broilers, while cartilage BMD decreased. It was consistent with the findings of Kobayashi et al. (2015). on articular cartilage thickness in young Beagles with spontaneous FHN. Moreover, in idiopathic avascular necrosis of the femoral head in children named Legg-Calvé-Perthes disease, similar thickening changes were observed in articular cartilage (Gershuni et al., 1978; Kim, 2011). Cartilage ECM consists of proteoglycan with swelling characteristics and a tension-resistant collagen fiber network, maintaining the structure and function of cartilage through the balance between proteoglycan and collagen fiber network (Moo et al., 2022; Alcaide-Ruggiero et al., 2023). The significant decrease of collagen content in cartilage in FHN broiler cartilage was found to precede changes in proteoglycan content. Consequently, the reduced restriction of the collagen fiber network on the swelling properties of proteoglycans may lead to cartilage swelling, potentially explaining variations in cartilage thickness and density. Another recent study showed that increased water content in damaged cartilage led to the reduction of cartilage density and the expansion of cartilage volume (Ciliberti et al., 2022). The elevated water content of cartilage in FHN broilers in this study may therefore corroborate the aforementioned findings. In addition, the serum content of the cartilage synthesis marker PIICP was notably elevated in FHS broilers compared to that of normal and FHSL broilers, indicating that in the initial stage of FHN, the body attempted to repair damaged cartilage by enhancing cartilage formation.

Articular cartilage, a smooth resilient tissue, serves the function of cushioning physiological pressures and maintaining a low-friction environment between adjacent bones (Wei et al., 2021). This study was the first attempt to elucidate the three-dimensional microstructure of FHN broiler cartilage. These findings revealed a notable increase in the surface roughness of cartilage, which was consistent with the observations of Seo et al. in articular cartilage in FHN humans (Seo et al., 2015). The research also indicated that in healthy broilers, the cartilage friction coefficient was as low as 0.003, similar to that in healthy human joints (Lin et al., 2021). However, in FHN broilers, both the cartilage friction and friction coefficient increased by tens of times, suggesting that the low-friction environment of the joints was

drastically altered with the development of FHN. Liao et al. (2022) concluded that cartilage surface roughness was significantly associated with a low-friction environment within the joint. Similarly, there was a strong positive correlation association between roughness, friction, and coefficient of friction in the present study. Doyran et al. (2017)concluded that cartilage modulus is a highly sensitive indicator in osteoarthritis, and the present study found a negative correlation between cartilage modulus and the degree of FHN, suggesting that cartilage modulus is likewise a sensitive indicator in FHN. In addition to a correlation between cartilage modulus and the severity of FHN, there was a significant correlation between cartilage friction force, friction coefficient, and stiffness, and the severity of FHN. These findings indicate that biomechanical changes in cartilage can be used as strong evidence for the progression of FHN in broilers.

The impact of bacteria on bone and cartilage in FHN-affected broilers cannot be ignored. In the present study, *S. aureus* was the most abundant bacteria isolated from the growth plate in broilers with FHN, followed by *Enterococcus* and *E. coli*. These opportunistic pathogens may translocate into the circulation of broilers through the respiratory, epidermis, and gastrointestinal tract (McNamee et al., 1999; Martin et al., 2011), subsequently colonizing osteochondrotic fissures or adhering to the cartilage matrix (Wideman, 2016). Collagen adhesin (**CNA**) is crucial for the adherence of cartilage by *S. aureus* and *Enterococcus*, with binding to collagen promoting the virulence potential of CAN on cartilage (Xu et al., 2004). A similar mechanism exists in bacterial adherence to bone (Montanaro et al., 1999). In addition, surface-associated material (**SAM**) from bacteria enhances bone resorption and osteoclast production, disrupting bone homeostasis (Wright et al., 2010) and potentially leading to a decline in bone quality. Huang et al. (2016) indicated that lipopolysaccharide (**LPS**) from Gram-negative bacteria such as *E. coli* is strongly associated with joint space narrowing. Smith et al. (1982) demonstrated that treatment of cartilage (Organoid culture in vitro) with *S. aureus* and *E. coli* resulted in abnormal degradation of glycosaminoglycans and chondrocyte death, suggesting that alterations of ECM in the cartilage of FHN-affected broilers may also be related to bacterial invasion.

Cell disintegration, abnormal mitochondrial accumulation, and oxidative stress damage were observed in chondrocytes in FHN broilers. The typical autophagosomes were found in FHS broiler chondrocytes, while abnormal mitochondrial accumulation was observed in FHSL chondrocytes. It was speculated that in the early stages of FHN, chondrocytes may maintain mitochondrial quality by eliminating damaged mitochondria via autophagy or mitophagy. However, as the disease progressed, dysfunction of autophagy and mitophagy led to the accumulation of redundant and damaged mitochondria in chondrocytes. Mitochondria are the primary sites of ROS production, and mitochondrial dysfunction leads to elevated intracellular ROS levels (Terkeltaub et al., 2002; Bolduc et al., 2019). Ferver et al. (2021) recently found that mitochondrial dysfunction occurs in the bone of broilers with bacterial chondronecrosis with osteomyelitis, also known as FHN (Jung et al., 2018; Ramser et al., 2023). In the present study, the significant increase in ROS levels in FHN chondrocytes implied that mitochondrial dysfunction may also be present in the chondrocytes of FHN broilers. Furthermore, previous studies have shown that the elevation of ROS levels exacerbates oxidative stress damage in chondrocytes, leading to chondrocyte damage and even apoptosis (Blanco et al., 2011). Chondrocytes are responsible for the synthesis of ECM components, which are mainly composed of proteoglycan and collagen fibers (Wei et al., 2021). In this study, both proteoglycan and collagen fiber content significantly decreased in FHSL broilers. Taken together, ECM alterations of cartilage in FHN broilers may be induced by chondrocyte damage from mitochondrial dysfunction, and mitochondrial dysfunction may be related to the pathogenesis of FHN (Ferver et al., 2021).

The alterations of cartilage ECM in the FHN broiler have notable features. It was that collagen fiber content significantly decreased in FHS broiler cartilage compared to healthy broilers, while proteoglycan content exhibited a significant reduction in FHSL broiler cartilage. These findings indicated that the collagen content of broiler cartilage changed significantly during the early stage of FHN. The changes in collagen are multifactorial results, involving not only alterations in collagen content but also disruption of collagen network structure and changes in individual collagen fibers (Temple-Wong et al., 2009; Moo et al., 2022). In the current investigation, a significant decrease in collagen fiber diameter and a loosening of the collagen fiber network structure occurred in cartilage in FHSL broilers. Overall, the collagen content of broiler cartilage significantly altered firstly during the development of FHN, followed by the decrease in collagen fiber diameter and the loosening of the collagen network structure, as well as a significant decrease in proteoglycan content. Shirazi et al. (2008) indicated that the collagen fiber network exerts a direct influence on cartilage biomechanics, thus the loosening of the collagen network in FHN broiler cartilage may be the main factor responsible for the alterations in cartilage biomechanical parameters.

Type II collagen is the main component of the cartilage. This study revealed that the number of col2a1-positive cells significantly decreased in FHN broiler cartilage, which was a reason for the decrease in collagen content. Cartilage collagen exhibits different birefringence in polarized light microscopy, with bright yellow or red representing type I collagen fibers, and green representing type III collagen fibers (Liu et al., 2021a). Our findings indicated that with the development of FHN, progressively more type III collagen fibers appeared, and type I collagen fibers were observed in the late stages of FHN. The role of Type III collagen fibers in cartilage damage remains controversial, as type I collagen fibers

have been observed in both healthy and damaged cartilage (Alcaide-Ruggiero et al., 2021). In contrast, type I collagen is produced in large quantities in osteoarthritic cartilage (Tschaikowsky et al., 2022), and thus it may be closely related to cartilage damage in FHN.

In summary, during the development of the spontaneous FHN, there was a progressive decrease in bone quality accompanied by joint space narrowing. Additionally, multifaceted damage was observed in the femoral head cartilage, primarily characterized by morphological changes, biomechanical functional disorders, oxidative stress damage in chondrocytes, and alterations in ECM. These parameters were closely associated with the severity of FHN in broilers.

ACKNOWLEDGMENTS

This work was supported by the National Natural Science Foundation of China (grant number 32273080).

DISCLOSURES

The authors declare no conflicts of interest.

REFERENCES

Alcaide-Ruggiero, L., R. Cugat, and J. M. Dominguez. 2023. Proteoglycans in articular cartilage and their contribution to chondral injury and repair mechanisms. Int J Mol Sci 24.

Alcaide-Ruggiero, L., V. Molina-Hernandez, M. M. Granados, and J. M. Dominguez. 2021. Main and minor types of collagens in the articular cartilage: the role of collagens in repair tissue evaluation in chondral defects. Int J Mol Sci 22.

Al-Rubaye, A. A. K., M. B. Couger, S. Ojha, J. F. Pummill, J. A. Koon, R. F. Wideman, and D. D. Rhoads. 2015. Genome analysis of staphylococcus agnetis, an agent of lameness in broiler chickens. Plos One 10:e0143336.

Alrubaye, A. A. K., N. S. Ekesi, A. Hasan, E. Elkins, S. Ojha, S. Zaki, S. Dridi, R. F. Wideman Jr., M. A. Rebollo, and D. D. Rhoads. 2020. Chondronecrosis with osteomyelitis in broilers: further defining lameness-inducing models with wire or litter flooring to evaluate protection with organic trace minerals. Poult Sci 99:5422–5429.

Blanco, F. J., I. Rego, and C. Ruiz-Romero. 2011. The role of mitochondria in osteoarthritis. Nat Rev Rheumatol 7:161–169.

Bolamperti, S., I. Villa, and A. Rubinacci. 2022. Bone remodeling: an operational process ensuring survival and bone mechanical competence. Bone Res 10:48.

Bolduc, J. A., J. A. Collins, and R. F. Loeser. 2019. Reactive oxygen species, aging and articular cartilage homeostasis. Free Radic Biol Med 132:73–82.

Brown, W. E., G. D. DuRaine, J. C. Hu, and K. A. Athanasiou. 2019. Structure-function relationships of fetal ovine articular cartilage. Acta Biomater 87:235–244.

Castro, F. L. S., L. Chai, J. Arango, C. M. Owens, P. A. Smith, S. Reichelt, C. DuBois, and A. Menconi. 2023. Poultry industry paradigms: Connecting the dots. J. Appl. Poult. Res. 32.

Chen, K., Y. Liu, J. He, N. Pavlos, C. Wang, J. Kenny, J. Yuan, Q. Zhang, J. Xu, and W. He. 2020. Steroid-induced osteonecrosis of the femoral head reveals enhanced reactive oxygen species and hyperactive osteoclasts. Int J Biol Sci 16:1888–1900.

Chen, Y., Y. Miao, K. Liu, F. Xue, B. Zhu, C. Zhang, and G. Li. 2022. Evolutionary course of the femoral head osteonecrosis: Histopathological - radiologic characteristics and clinical staging systems. J Orthop Translat 32:28–40.

Ciliberti, F. K., G. Cesarelli, L. Guerrini, A. E. Gunnarsson, R. Forni, R. Aubonnet, M. Recenti, D. Jacob, H. Jonsson Jr., V. Cangiano, A. S. Islind, M. Gambacorta, and P. Gargiulo. 2022. The role of bone mineral density and cartilage volume to predict knee cartilage degeneration. Eur J Transl Myol 32.

Dinev, I. 2009. Clinical and morphological investigations on the prevalence of lameness associated with femoral head necrosis in broilers. Br Poult Sci 50:284–290.

Dinev, I., D. Kanakov, I. Kalkanov, S. Nikolov, and S. Denev. 2019. Comparative pathomorphologic studies on the incidence of fractures associated with leg skeletal pathology in commercial broiler chickens. Avian Dis 63:641–650.

Dong, S., L. Li, F. Hao, Z. Fang, R. Zhong, J. Wu, and X. Fang. 2024. Improving quality of poultry and its meat products with probiotics, prebiotics, and phytoextracts. Poult Sci 103:103287.

Doyran, B., W. Tong, Q. Li, H. Jia, X. Zhang, C. Chen, M. Enomoto-Iwamoto, X. L. Lu, L. Qin, and L. Han. 2017. Nanoindentation modulus of murine cartilage: A sensitive indicator of the initiation and progression of post-traumatic osteoarthritis. Osteoarthritis Cartilage 25:108–117.

Durairaj, V., R. Okimoto, K. Rasaputra, F. D. Clark, and N. C. Rath. 2009. Histopathology and serum clinical chemistry evaluation of broilers with femoral head separation disorder. Avian Dis 53:21–25.

Elgaz, S., H. Bonig, and P. Bader. 2020. Mesenchymal stromal cells for osteonecrosis. J. Transl. Med. 18:399.

Fan, R., K. Liu, and Z. Zhou. 2021. Abnormal lipid profile in fast-growing broilers with spontaneous femoral head necrosis. Front. Physiol. 12:685968.

Farizqi, M. T. I., M. H. Effendi, R. T. S. Adikara, I. S. Yudaniayanti, G. D. S. Putra, A. R. Khairullah, S. C. Kurniawan, O. S. M. Silaen, S. Ramadhani, S. K. Millannia, S. E. Kaben, and Y. K. K. Waruwu. 2023. Detection of extended-spectrum β-lactamase-producing escherichia coli genes isolated from cat rectal swabs at surabaya veterinary hospital, Indonesia. Vet. World 16:1917–1925.

Ferver, A., E. Greene, R. Wideman, and S. Dridi. 2021. Evidence of mitochondrial dysfunction in bacterial chondronecrosis with osteomyelitis-affected broilers. Front Vet Sci 8:640901.

Gershuni, D. H., A. Axer, and D. J. J. Hendel. 1978. Arthrographic findings in legg-calvé-perthes disease and transient synovitis of the hip. J. Bone Joint Surg. Am. 60:457–464.

Girijan, S. K., and D. Pillai. 2021. Identification and characterization of vancomycin-resistantstaphylococcus aureusin hospital wastewaters: evidence of horizontal spread of antimicrobial resistance. J. Water and Health 19:785–795.

Granquist, E. G., G. Vasdal, I. C. de Jong, and R. O. Moe. 2019. Lameness and its relationship with health and production measures in broiler chickens. Animal 13:2365–2372.

Grupioni, N. V., V. A. Cruz, N. B. Stafuzza, L. A. Freitas, S. B. Ramos, R. P. Savegnago, J. O. Peixoto, M. C. Ledur, and D. P. Munari. 2015. Phenotypic, genetic and environmental parameters for traits related to femur bone integrity and body weight at 42 days of age in a broiler population. Poult Sci 94:2604–2607.

Guerado, E., and E. Caso. 2016. The physiopathology of avascular necrosis of the femoral head: an update. Injury 47(Suppl 6):S16–S26.

Guo, J. B., T. Liang, Y. J. Che, H. L. Yang, and Z. P. Luo. 2020. Structure and mechanical properties of high-weight-bearing and low-weight-bearing areas of hip cartilage at the micro- and nano-levels. BMC Musculoskelet Disord 21:425.

Hines, J. T., W. L. Jo, Q. Cui, M. A. Mont, K. H. Koo, E. Y. Cheng, S. B. Goodman, Y. C. Ha, P. Hernigou, L. C. Jones, S. Y. Kim, T. Sakai, N. Sugano, T. Yamamoto, M. S. Lee, D. Zhao, W. Drescher, T. Y. Kim, Y. K. Lee, B. H. Yoon, S. H. Baek, W. Ando, H. S. Kim, and J. W. Park. 2021. Osteonecrosis of the femoral head: an updated review of arco on pathogenesis, staging and treatment. J Korean Med Sci 36:e177.

Huang, Z. Y., T. Stabler, F. X. Pei, and V. B. Kraus. 2016. Both systemic and local lipopolysaccharide (lps) burden are associated with knee oa severity and inflammation. Osteoarthritis Cartilage 24:1769–1775.

Jung, A., L. R. Chen, M. M. Suyemoto, H. J. Barnes, and L. B. Borst. 2018. A review of enterococcus cecorum infection in poultry. Avian Dis 62:261–271.

Kang, P., H. Gao, F. Pei, B. Shen, J. Yang, and Z. Zhou. 2010. Effects of an anticoagulant and a lipid-lowering agent on the prevention of steroid-induced osteonecrosis in rabbits. Int. J. Exp. Pathol. 91:235–243.

Kense, M. J., and W. J. M. Landman. 2011. Enterococcus cecoruminfections in broiler breeders and their offspring: molecular epidemiology. Avian Pathol. 40:603–612.

Kim, H. K. J. J. o. P. O. 2011. Legg-calve-perthes disease: etiology, pathogenesis, and biology. Pages S141-S146.

Kobayashi, R., T. Kurotaki, N. Yamada, S. Kumabe, T. Doi, Y. Wako, and M. Tsuchitani. 2015. Spontaneous and bilateral necrosis of the femoral head in a young experimental beagle dog. J Toxicol Pathol 28:121–124.

Kolakshyapati, M., R. J. Flavel, T. Z. Sibanda, D. Schneider, M. C. Welch, and I. Ruhnke. 2019. Various bone parameters are positively correlated with hen body weight while range access has no beneficial effect on tibia health of free-range layers. Poult. Sci. 98:6241–6250.

Kuettner, K. E., and A. A. Cole. 2005. Cartilage degeneration in different human joints. Osteoarthritis Cartilage 13:93–103.

Kuroshima, S., M. Kaku, T. Ishimoto, M. Sasaki, T. Nakano, and T. Sawase. 2017. A paradigm shift for bone quality in dentistry: a literature review. J Prosthodont Res 61:353–362.

Lawrence, A., X. Xu, M. D. Bible, S. Calve, C. P. Neu, and A. Panitch. 2015. Synthesis and characterization of a lubricin mimic (mlub) to reduce friction and adhesion on the articular cartilage surface. Biomaterials 73:42–50.

Li, M., H. Yin, Z. Yan, H. Li, J. Wu, Y. Wang, F. Wei, G. Tian, C. Ning, H. Li, C. Gao, L. Fu, S. Jiang, M. Chen, X. Sui, S. Liu, Z. Chen, and Q. Guo. 2022. The immune microenvironment in cartilage injury and repair. Acta Biomater 140:23–42.

Li, Z., W. Shao, X. Lv, B. Wang, L. Han, S. Gong, P. Wang, and Y. Feng. 2023. Advances in experimental models of osteonecrosis of the femoral head. J. Orthop. Translat. 39:88–99.

Liao, J., X. Liu, S. Miramini, L. J. C. i. B. Zhang, and Medicine. 2022. Influences of variability and uncertainty in vertical and horizontal surface roughness on articular cartilage lubrication. 148:105904.

Lilburn, M. S., K. Ngiam-Rilling, and D. J. Myers-Miller. 1989. Growth and development of broiler breeders. 2. Independent effects of dietary formulation versus body weight on skeletal and muscle growth. Poult. Sci. 68:1274–1281.

Liu, J., M. Y. Xu, J. Wu, H. Zhang, L. Yang, D. X. Lun, Y. C. Hu, and B. Liu. 2021a. Picrosirius-polarization method for collagen fiber detection in tendons: a mini-review. Orthop. Surg. 13:701–707.

Lin, W., and J. Klein. 2021. Recent progress in cartilage lubrication. Adv. Mater. 33:e2005513.

Liu, K., R. Fan, and Z. Zhou. 2021b. Endoplasmic reticulum stress, chondrocyte apoptosis and oxidative stress in cartilage of broilers affected by spontaneous femoral head necrosis. Poult. Sci. 100:101258, doi:10.1016/j.psj.2021.101258.

Liu, K., K. Wang, L. Wang, and Z. Zhou. 2021c. Changes of lipid and bone metabolism in broilers with spontaneous femoral head necrosis. Poult. Sci. 100:100808.

Liu, K. L., Y. F. He, B. W. Xu, L. X. Lin, P. Chen, M. K. Iqbal, K. Mehmood, and S. C. Huang. 2023. Leg disorders in broiler chickens: a review of current knowledge. Anim Biotechnol 34:5124–5138.

Ma, C., T. Du, X. Niu, and Y. Fan. 2022. Biomechanics and mechanobiology of the bone matrix. Bone Res 10:59.

Martin, L. T., M. P. Martin, and H. J. J. A. d. Barnes. 2011. Experimental reproduction of enterococcal spondylitis in male broiler breeder chickens. 55:273-278.

McNamee, P. T., J. J. McCullagh, J. D. Rodgers, B. H. Thorp, H. J. Ball, T. J. Connor, D. McConaghy, and J. A. Smyth. 1999. Development of an experimental model of bacterial chondronecrosis with osteomyelitis in broilers following exposure to staphylococcus aureus by aerosol, and inoculation with chicken anaemia and infectious bursal disease viruses. Avian Pathol 28:26–35.

McNamee, P. T., and J. A. Smyth. 2000. Bacterial chondronecrosis with osteomyelitis ('femoral head necrosis') of broiler chickens: a review. Avian Pathol 29:477–495.

Montanaro, L., C. R. Arciola, L. Baldassarri, and E. J. B. Borsetti. 1999. Presence and expression of collagen adhesin gene (cna) and slime production in staphylococcus aureus strains from orthopaedic prosthesis infections. Biomaterials 20:1945–1949.

Moo, E. K., M. Ebrahimi, S. C. Sibole, P. Tanska, and R. K. Korhonen. 2022. The intrinsic quality of proteoglycans, but not collagen fibres, degrades in osteoarthritic cartilage. Acta Biomater 153:178–189.

Murphey, M. D., K. L. Foreman, M. K. Klassen-Fischer, M. G. Fox, E. M. Chung, and M. J. J. R. Kransdorf. 2014. From the radiologic pathology archives imaging of osteonecrosis: radiologic-pathologic correlation. 34:1003-1028.

Nagai, M., T. Aoyama, A. Ito, J. Tajino, H. Iijima, S. Yamaguchi, X. Zhang, and H. Kuroki. 2015. Alteration of cartilage surface collagen fibers differs locally after immobilization of knee joints in rats. J Anat 226:447–457.

Nobakhti, S., and S. J. Shefelbine. 2018. On the relation of bone mineral density and the elastic modulus in healthy and pathologic bone. Curr Osteoporos Rep 16:404–410.

Packialakshmi, B., N. C. Rath, W. E. Huff, and G. R. Huff. 2015. Poultry femoral head separation and necrosis: a review. Avian Dis 59:349–354.

Pal, P., R. Bhatta, R. Bhattarai, P. Acharya, S. Singh, and A. D. Harries. 2022. Antimicrobial resistance in bacteria isolated from the poultry production system in nepal. Public Health Action 12:165–170.

Paz, I. C. d. L. A., A. A. Mendes, M. Martins, B. Fernandes, I. Almeida, E. Milbradt, A. Balog, and C. Komiyama. 2009. Follow-up of the development of femoral degeneration lesions in broilers.

Petek, D., D. Hannouche, and D. Suva. 2019. Osteonecrosis of the femoral head: Pathophysiology and current concepts of treatment. EFORT Open Rev 4:85–97.

Quan, H., C. Ren, Y. He, F. Wang, S. Dong, and H. Jiang. 2023. Application of biomaterials in treating early osteonecrosis of the femoral head: Research progress and future perspectives. Acta Biomater 164:15–73.

Ramser, A., R. Hawken, E. Greene, R. Okimoto, B. Flack, C. J. Christopher, S. R. Campagna, and S. Dridi. 2023. Bone metabolite profile differs between normal and femur head necrosis (fhn/bco)-affected broilers: Implications for dysregulated metabolic cascades in fhn pathophysiology. Metabolites 13:662.

Saeki Fernandes, A., C. C. N. Fonseca, G. Rodrigues da Silva Sasso, L. Carvalho Cezar, M. Aparecida Dos Santos, M. J. Simoes, R. S. Simoes, and R. Florencio-Silva. 2018. Combined effects of ovariectomy and streptozotocin-induced diabetes in the articular cartilage of rats. Climacteric 21:75–81.

Schmitz, N., S. Laverty, V. B. Kraus, and T. Aigner. 2010. Basic methods in histopathology of joint tissues. Osteoarthritis Cartilage 18(Suppl 3):S113–S116.

Seo, E. M., S. K. Shrestha, C. T. Duong, A. R. Sharma, T. W. Kim, A. Vijayachandra, M. S. Thompson, M. G. Cho, S. Park, K. Kim, S. Park, and S. S. Lee. 2015. Tribological changes in the articular cartilage of a human femoral head with avascular necrosis. Biointerphases 10:021004.

Sgavioli, S., E. T. Santos, L. L. Borges, G. M. Andrade-Garcia, D. M. C. Castiblanco, V. R. Almeida, R. G. Garcia, A. C. Shimano, I. A. Naas, and S. M. Baraldi-Artoni. 2017. Effect of the addition of glycosaminoglycans on bone and cartilaginous development of broiler chickens. Poult Sci 96:4017–4025.

Shirazi, R., A. Shirazi-Adl, and M. Hurtig. 2008. Role of cartilage collagen fibrils networks in knee joint biomechanics under compression. J Biomech 41:3340–3348.

Smith, R. L., T. C. Merchant, D. J. J. A. Schurman, and R. O. J. O. T. A. C. O. Rheumatology. 1982. In vitro cartilage degradation by escherichia coli and staphylococcus aureus. 25:441-446.

Sun, Y., D. R. Mauerhan, J. S. Kneisl, H. J. Norton, N. Zinchenko, J. Ingram, E. N. Hanley Jr, and H. E. J. T. O. R. J. Gruber. 2012. Histological examination of collagen and proteoglycan changes in osteoarthritic menisci. 6:24.

Singh, M., B. Singh, K. Sharma, N. Kumar, S. Mastana, and P. Singh. 2023. A molecular troika of angiogenesis, coagulopathy and endothelial dysfunction in the pathology of avascular necrosis of femoral head: a comprehensive review. Cells 12:2278.

Szafraniec, G. M., P. Szeleszczuk, and B. Dolka. 2022. Review on skeletal disorders caused by *staphylococcus* spp. in poultry. Vet. Q 42:21–40.

Tan, B., W. Li, P. Zeng, H. Guo, Z. Huang, F. Fu, H. Gao, R. Wang, and W. Chen. 2021. Epidemiological study based on china osteonecrosis of the femoral head database. Orthop Surg 13:153–160.

Temple-Wong, M. M., W. C. Bae, M. Q. Chen, W. D. Bugbee, D. Amiel, R. D. Coutts, M. Lotz, and R. L. Sah. 2009. Biomechanical, structural, and biochemical indices of degenerative and osteoarthritic deterioration of adult human articular cartilage of the femoral condyle. Osteoarthritis Cartilage 17:1469–1476.

Terkeltaub, R., K. Johnson, A. Murphy, and S. J. M. Ghosh. 2002. Invited review: the mitochondrion in osteoarthritis. 1:301-319.

Tschaikowsky, M., S. Brander, V. Barth, R. Thomann, B. Rolauffs, B. N. Balzer, and T. Hugel. 2022. The articular cartilage surface is impaired by a loss of thick collagen fibers and formation of type i collagen in early osteoarthritis. Acta Biomater 146:274–283.

Wang, C., H. Meng, Y. Wang, B. Zhao, C. Zhao, W. Sun, Y. Zhu, B. Han, X. Yuan, R. Liu, X. Wang, A. Wang, Q. Guo, J. Peng, and S. Lu. 2018. Analysis of early stage osteonecrosis of the human femoral head and the mechanism of femoral head collapse. Int. J. Biol. Sci. 14:156–164.

Wang, F., L. Zheng, J. Theopold, S. Schleifenbaum, C. E. Heyde, and G. Osterhoff. 2022. Methods for bone quality assessment in human bone tissue: a systematic review. J Orthop Surg Res 17:174.

Wei, W., and H. Dai. 2021. Articular cartilage and osteochondral tissue engineering techniques: recent advances and challenges. Bioact Mater 6:4830–4855.

Weimer, S. L., R. F. Wideman, C. G. Scanes, A. Mauromoustakos, K. D. Christensen, and Y. Vizzier-Thaxton. 2021. Impact of experimentally induced bacterial chondronecrosis with osteomyelitis (BCO) lameness on health, stress, and leg health parameters in broilers. Poult. Sci. 100:101457.

Wideman, R. F. 2016. Bacterial chondronecrosis with osteomyelitis and lameness in broilers: a review. Poult. Sci. 95:325–344.

Wright, J. A., and S. P. Nair. 2010. Interaction of staphylococci with bone. Int. J. Med. Microbiol. 300:193–204.

Xu, T., K. Yue, C. Zhang, X. Tong, L. Lin, Q. Cao, and S. Huang. 2022. Probiotics treatment of leg diseases in broiler chickens: a review. Probiotics Antimicrob Proteins 14:415–425.

Xu, Y., J. M. Rivas, E. L. Brown, X. Liang, and M. J. T. J. O. I. D. Höök. 2004. Virulence potential of the staphylococcal adhesin cna in experimental arthritis is determined by its affinity for collagen. 189:2323-2333.

Yu, Y., Y. Jiang, H. Ge, X. Fan, H. Gao, and Z. Zhou. 2024. Hif-1alpha in cartilage homeostasis, apoptosis, and glycolysis in mice with steroid-induced osteonecrosis of the femoral head. J. Cell Physiol 239: e31224.

Yu, Y., S. Wang, and Z. Zhou. 2020. Cartilage homeostasis affects femoral head necrosis induced by methylprednisolone in broilers. Int. J. Mol. Sci. 21:4841.

Zhang, M., S. Li, K. Pang, and Z. Zhou. 2019. Endoplasmic reticulum stress affected chondrocyte apoptosis in femoral head necrosis induced by glucocorticoid in broilers. Poult. Sci. 98:1111–1120.

Zhao, C., G. Liu, Y. Zhang, G. Xu, X. Yi, J. Liang, Y. Yang, J. Liang, C. Ma, Y. Ye, M. Yu, and X. Qu. 2020a. Association between serum levels of bone turnover markers and bone mineral density in men and women with type 2 diabetes mellitus. J. Clin. Lab Anal. 34:e23112.

Zhao, D., F. Zhang, B. Wang, B. Liu, L. Li, S. Y. Kim, S. B. Goodman, P. Hernigou, Q. Cui, W. C. Lineaweaver, J. Xu, W. R. Drescher, and L. Qin. 2020b. Guidelines for clinical diagnosis and treatment of osteonecrosis of the femoral head in adults (2019 version). J. Orthop. Translat. 21:100–110.

Zuidhof, M. J., B. L. Schneider, V. L. Carney, D. R. Korver, and F. E. Robinson. 2014. Growth, efficiency, and yield of commercial broilers from 1957, 1978, and 2005. Poult. Sci. 93:2970–2982.